Clin Neuroradiol (2019) 29:797–804
https://doi.org/10.1007/s00062-019-00849-2

CLINICAL CASE

Freiburg Neuropathology Case Conference

A Progressive Lesion of the Optic Tract, Brainstem, Hypothalamus and Basal Ganglia

C. A. Taschner[1] · S. Doostkam[2] · P. C. Reinacher[3] · H. Urbach[1] · A. Rau[1] · M. Prinz[2]

Published online: 8 November 2019

Case Report

A 63-year-old male patient presented with a 6-month history of reduction in performance and fatigue as well as a change in character and for 3 months he had an additional deterioration in vigilance with an increasing imperative urge to sleep and a frontal disinhibition, which led to admission to psychiatry. Magnetic resonance imaging (MRI) revealed a suspicious lesion of the right optic tract and the hypothalamus (Figs. 1 and 2). A stereotactic biopsy in the area of the right hypothalamus above the optic tract was performed, revealing only small cell groups of B and T cells , which were considered non-specific; however, the patient had been under corticotherapy in the month prior to the biopsy and 2 months later the patient presented in a clinically stable condition and the corticotherapy had been discontinued. On MRI new lesions had occurred (Figs. 3 and 4) located bilaterally in the basal ganglia and a second stereotactic biopsy was performed targeting out a contrast-enhancing lesion in the left globus pallidus (Fig. 5).

Figs. 1 and 2 relate to the MRI performed before the 1st stereotactic biopsy.

Figs. 3 and 4 are related to the MRI performed before the second stereotactic biopsy.

Imaging

Fluid-attenuated inversion recovery (FLAIR) images obtained on the initial presentation of the patient showed hyperintense changes of signal intensities extending from the temporal white matter (Fig. 1a, d, arrowhead), the mesencephalon (Fig. 1a, arrowhead), the hypothalamus (Fig. 1b, arrowhead) and the crus of the cerebrum (Fig. 1b, arrow), along to the basal ganglia (Fig. 1c, arrowhead; Fig. 1d, arrow) up to the anteromedial parts of the thalamus (Fig. 1d, arrowhead). On T1-weighted non-contrast images local thickening of the optic chiasm as well as the right optic tract was observed (Fig. 2a, arrowhead). On T1-weighted images after i.v. administration of gadolinium this lesion revealed marked and homogeneous contrast enhancement (Fig. 2b, c, arrowhead). The MR images obtained 2 months after the first non-conclusive stereotactic biopsy showed a marked increase of the hyperintense changes of signal intensities on FLAIR images (Fig. 3, arrowhead). On T1-weighted non-contrast images hyperintense changes of the hypothalamus have occurred (Fig. 4a, b, arrow), which displayed some degree of contrast enhancement on T1-weighted postcontrast images (Fig. 4b, arrowhead). The local thickening of the right optic tract was clearly regressing (not shown).

Differential Diagnosis

Neurosarcoidosis

Sarcoidosis is a systemic granulomatous inflammatory disease of unknown etiology with an incidence of up to 10 per 100,000 patients. Sarcoidosis usually clinically affects the lungs and the skin. Around 5% of the patients show clinical symptoms of central nervous system (CNS) involvement [1, 2] but cerebral affection is confirmed by autopsy in up to 25% of sarcoidosis patients. In MRI typ-

✉ C. A. Taschner
christian.taschner@uniklinik-freiburg.de

1 Department of Neuroradiology, Medical Centre, University of Freiburg, Freiburg, Germany

2 Department of Neuropathology, Medical Centre, University of Freiburg, Freiburg, Germany

3 Department of Stereotactic and Functional Neurosurgery, Medical Centre, University of Freiburg, Freiburg, Germany

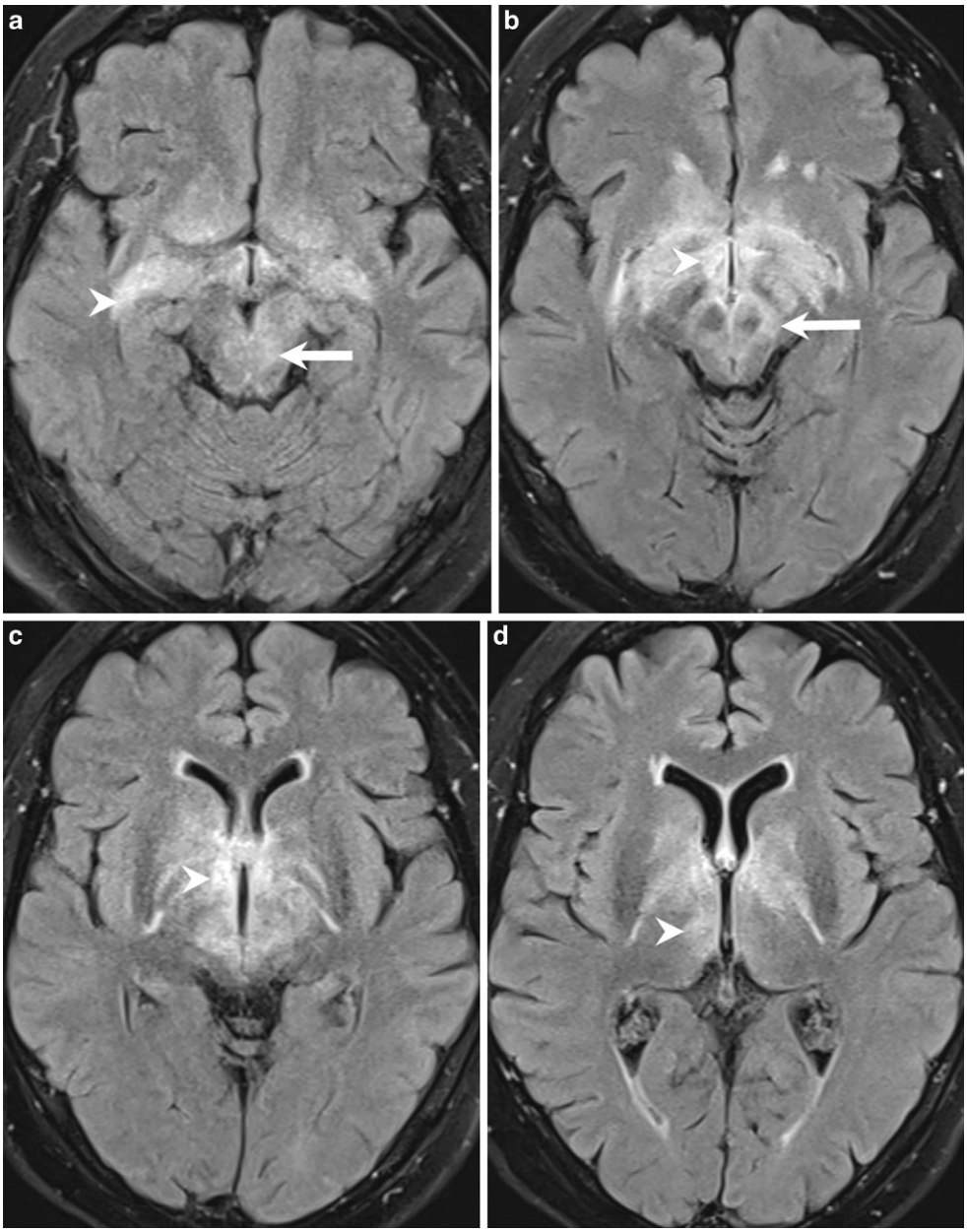

Fig. 1 Axial fluid-attenuated inversion recovery (FLAIR) images obtained on the initial presentation of the patient show hyperintense changes of signal intensities extending from the temporal white matter (**a**, *arrowhead*), the mesencephalon (**a**, *arrow*), the hypothalamus (**b**, *arrowhead*) and the crus of the cerebrum (**b**, *arrow*), along to the basal ganglia (**c**, *arrowhead*) up to the anteromedial parts of the thalamus (**d**, *arrowhead*)

ical features of neurosarcoidosis can be identified in every tenth patient [1]. Neurosarcoidosis preferentially occurs in male patients and mean onset is within the fourth decade of life. Most patients present with a cranial neuropathy, in particular Bell's palsy due to affection of the facial nerve (23–73%) [1]. Many other neurological symptoms can be caused by neurosarcoidosis depending on the location of the lesions. In imaging, basal leptomeningeal spread is the most common feature of neurosarcoidosis presenting as a meningeal thickening with diffuse or nodular enhancement after gadolinium administration and T1/T2-hypointense material in the subarachnoid spaces. Also, affection along the perivascular spaces is frequent. Typical patterns of parenchymal involvement are solitary mass lesions (15%), multiple small enhancing lesions (in around 35%) as well as periventricular T2-hyperintense changes (50%). The optic chiasm, the hypothalamus and the infundibulum are preferably affected. Small infarctions may occur due to vasculitic changes caused by neurosarcoidosis. Complications include obstructive hydrocephalus [2]. Steroids are commonly used as first line treatment of sarcoid and can alter the results of imaging, especially reducing contrast enhancement [2]. In the present case, neurosarcoidosis is a relatively probable differential diagnosis since both the initial nodular hypothalamic/chiasmal enhancing lesion as well as the FLAIR hyperintensities along the perivascular spaces and the basal ganglia are commonly seen in neurosarcoidosis.

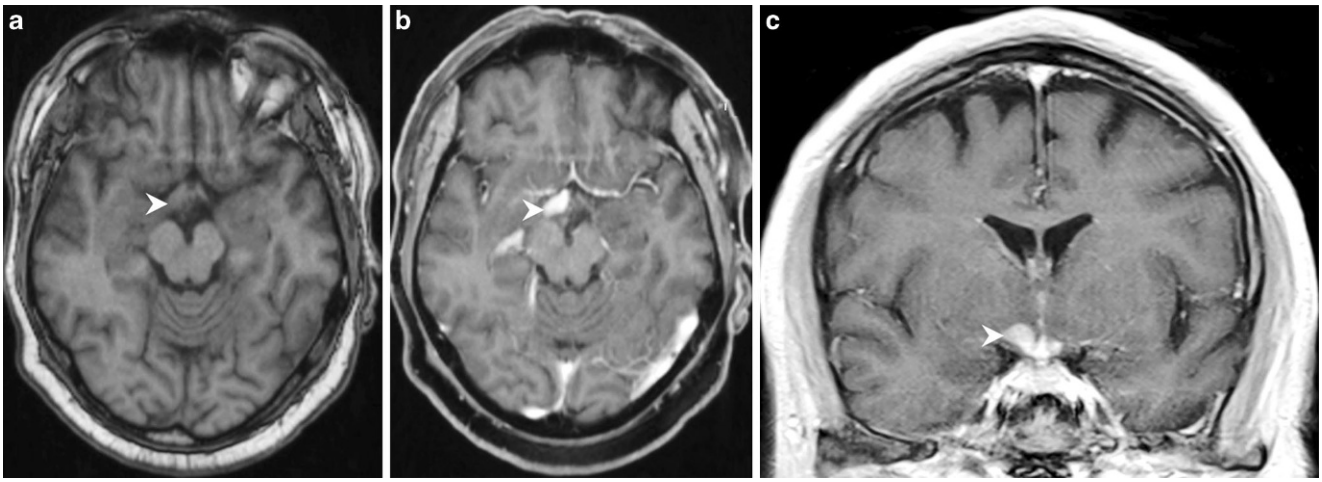

Fig. 2 On axial T1-weighted non-contrast images (**a**) local thickening of the optic chiasm as well as the right optic tract (**a**, *arrowhead*) can be observed. On axial (**b**) and coronal (**c**) T1-weighted images after i.v. administration of gadolinium this lesion reveals marked and homogeneous contrast enhancement (**b, c**, *arrowhead*)

Whipple's Disease

Whipple's disease (WD) is an extremely rare systemic infection with the actinomycete *Tropheryma whipplei* causing various intestinal and extraintestinal symptoms. Cerebral affection of WD occurs in 33% of systemic infections and is seen especially in men between the ages of 30 and 60 years [3]. Isolated CNS manifestations are rare. Clinically, CNS WD shows no specific features, while hypothalamic manifestations are described. In the literature, multiple case reports lead to an inhomogeneous imaging pattern of cerebral manifestation of WD. The WD lesions are usually T2-hyperintense and show a relatively symmetrical distribution pattern. There seems to be a predilection for the basal telencephalon, thalamus, hypothalamus and midbrain [3]. Focal and/or nodular inhomogeneous gadolinium enhancing lesions, including in the hypothalamus, are described as well [3]. In the present case, WD was a differential diagnosis, since perivascular changes of the basal ganglia and singular nodular enhancing lesions were seen.

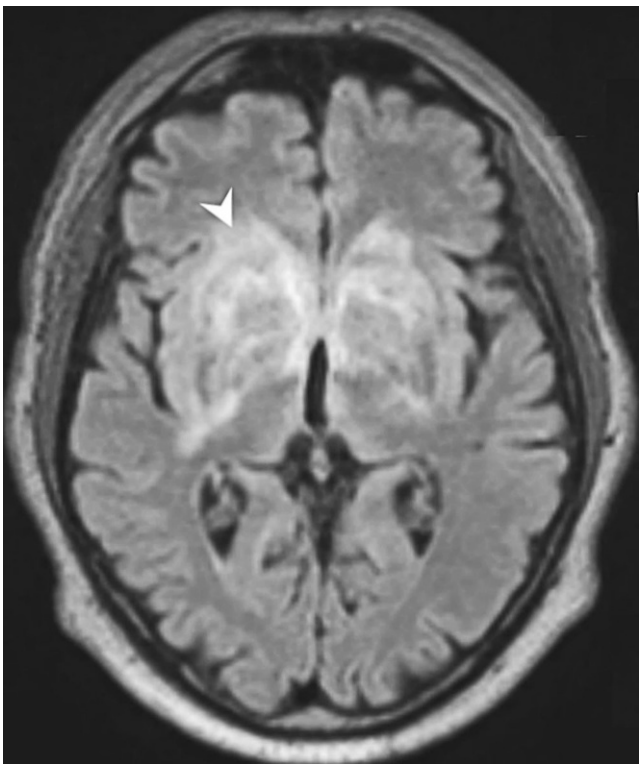

Fig. 3 MR image obtained 2 months after the first inconclusive stereotactic biopsy show a marked increase of the hyperintense changes of signal intensities on axial FLAIR images (*arrowhead*)

Primary CNS Lymphoma

Approximately 7% of primary intracranial neoplasms are primary CNS lymphomas (PCNSL). Of these 98% are diffuse large B-cell non-Hodgkin lymphomas. In immunocompetent patients, the highest incidence is seen around the age of 60 years, while in immunocompromised patients a peak in the incidence is observed towards the end of the fourth decade. Patients typically present with altered mental status and focal neurological deficits [4]. In MRI, the PCNSL is a relatively well-delimited, mostly cortex isointense or hypointense and strongly contrast-enhancing lesion with a mass effect. In patients with impaired immune function, a peripheral enhancement pattern after gadolinium administration with central necrosis rather than a homogeneous contrast enhancement is frequently observed. A diffusion restriction of the mass as well as a native hyperdensity in the cranial CT is common [5]. Approximately 60–80% of primary CNS lymphomas are supratentorial, involving the basal ganglia in up to 10%. The callosal body is sometimes

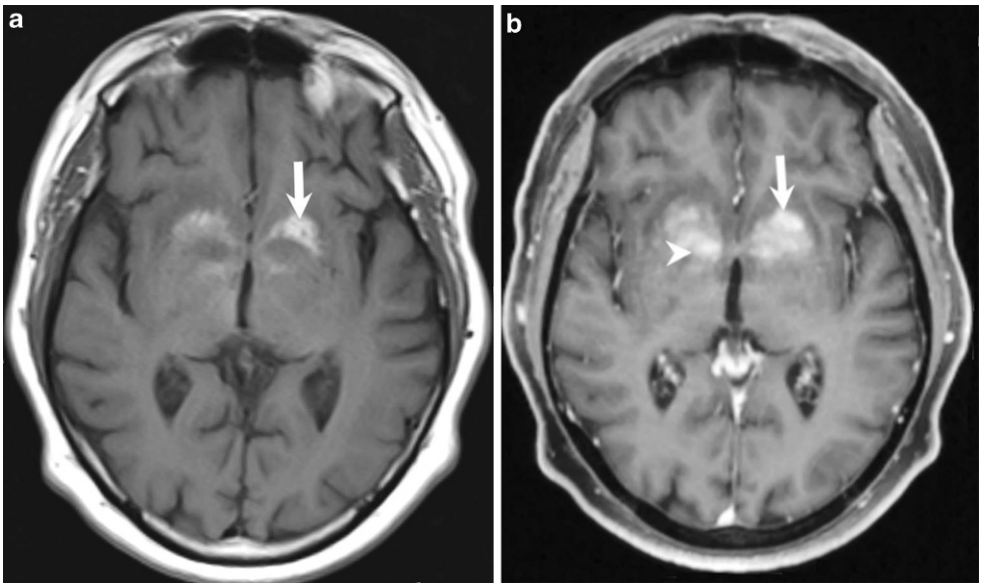

Fig. 4 On axial T1-weighted non-contrast images hyperintense changes of the basal ganglia are seen (**a, b**, *arrow*). In addition the basal ganglia display some degree of bilateral contrast enhancement on axial T1-weighted post contrast images (**b**, *arrowhead*)

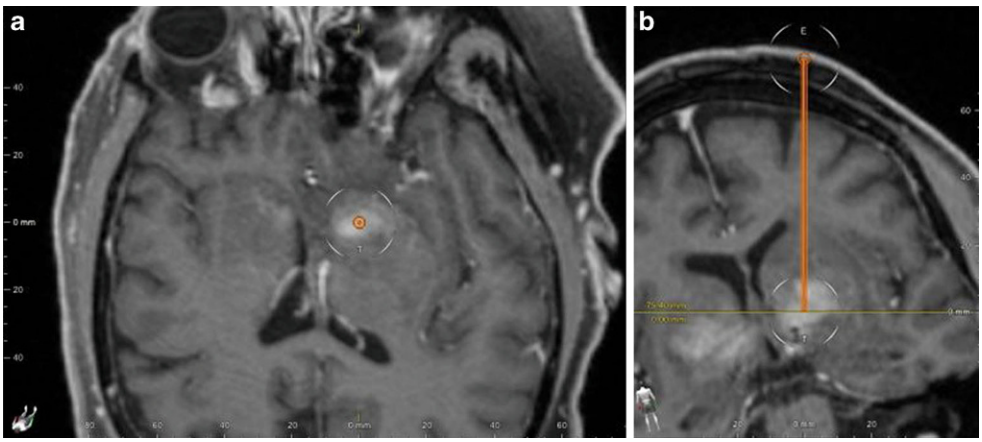

Fig. 5 Planned trajectory for the second stereotactic biopsy. T1-weighted, contrast enhanced MRI (magnetic resonance imaging) with the probes eye view in the target point (**a**) and the trajectory in the coronal plane (**b**)

affected and a subependymal spread is observed. Secondary leptomeningeal spread is found in about every third PCNSL patient. In immunocompromised patients, focal hemorrhages are described [4]. In the present case, the initially non-contrast-enhancing sections described previously were rather atypical for PCNSL. This discrepancy might be explained by previous steroid therapy, since this can significantly alter imaging features and especially contrast enhancement.

Angiocentric Lymphoma

Angiocentric lymphomas have to be distinguished from primary CNS lymphomas. Intravascular lymphoma (IVL) is a rare entity of diffuse large B-cell lymphoma with predilection for capillaries, venules, arterioles and small arteries [6]. It particularly affects patients around the age of 60 to 65 years and causes mainly skin and CNS symptoms, but can involve any organ. Cutaneous manifestations include plaques and nodular lesions and the most common neurological symptom is a progressive dementia while focal neurological deficits are rarer but also observed [7]. In MRI, multifocal T2-hyperintense and T1-hypointense lesions of the deep white matter, cortex or basal ganglia with partial blood-brain barrier disruptions are often described [8]. The lesions can be caused by both vasogenic edema and/or gliosis and a hemorrhagic transformation is possible. In 36%, infarct-like lesions with a strong diffusion restriction are also evident. Some cases showed meningeal affection or focal mass lesions. In contrast to the PCNSL, the lesions of the IVL in native computed tomography are hypodense [6, 7]. From the imaging aspect, the presented case was primarily suspected of being an angiocentric lymphoma due to the solitary enhancing mass and diffuse T2-hyperintensities of the basal ganglia; however, the lack of affection of the peripheral parenchyma and the symmetrical distribution pattern are not typical.

Diffuse Astrocytoma

Diffuse astrocytoma is a well-differentiated, slowly growing (WHO grade II) but infiltrating neoplasm with a certain tendency to degenerate to anaplastic astrocytoma (WHO grade III). The most common location is supratentorial (two thirds) involving the white matter of frontal and temporal lobes. Extended growth into the cortex is possible. Of diffuse astrocytomas one third are located infratentorially with the majority in the brainstem (50% of brainstem gliomas are diffuse astrocytomas). Diffuse astrocytomas account for 9% of all glioma cases and the majority occur in younger adults between 20 and 45 years of age, with a slight male predominance. In childhood it is the second most common astrocytoma after pilocytic astrocytoma. In MRI diffuse astrocytoma presents as a homogeneous T1 hypointense, T2 and FLAIR hyperintense expanding mass of the white matter and adjacent cortex. Sometimes it seems to be circumscribed, but as described by the name "diffuse", it grows by infiltration. Detection of enhancing parts should be interpreted as progression to a higher grade [9]. In the present case, the juxtaposition of infiltrative T2-hyperintense lesions and circumscribed nodular contrast-enhancing lesions as well as the rapid progression to an overall enhancing lesion with focal hemorrhage, might be compatible with a dedifferentiated higher grade diffuse astrocytoma.

Histology

The results of the histopathological and immunohistochemical examinations of the first stereotactic biopsy were not clearly groundbreaking. Calcified material (primarily bone meal), coagulated blood, fibrin, gliotic and edematous CNS tissue, and necrotic material were found in the small samples. Within one of the small samples a marginally small cell group consisting of mononuclear cells with a round nucleus, partly with artificial changes, could be identified (Fig. 6). Immunohistochemically, mixed B and T cell infiltrates were detected in the CD20 and CD3 reactions. Clear mitosis figures were not detectable here. However, the proliferation rate in the MIB1 (Ki67) immunohistochemistry was very high with almost all cell nuclei labeled positively. For this reason, parts of a lymphomatoid lesion not completely captured here could not be excluded with certainty. Unusually, however, was the mixed-cell character of the infiltrates, so that an inflammatory process should also be discussed as a differential diagnosis. Multinucleated giant cells as a sign of granulomatous inflammation could not be detected here. There was also no evidence for a granulocytic purulent inflammation in the material. Further immunohistochemical or molecular-pathological investigations (such as a clonality analysis) were not possible, as the material was completely consumed due to the very small dimension. The reference pathology of this biopsy by the network for lymphoma and lymphoid lesions of the nervous system (NLLLN) Cologne did also not reveal new aspects, so that a clear diagnosis of the material did not seem possible. Fig. 6 relates to specimens from the first stereotactic biopsy.

The pathological process was then stereotactically biopsied about 10 weeks later again. In the second stereotactic biopsy, large blastic cells were already visible intraoperatively, so that the suspected diagnosis of a lymphoma was made here. The histopathological preparations of the formalin-fixed material also showed infiltrates of a cell-rich

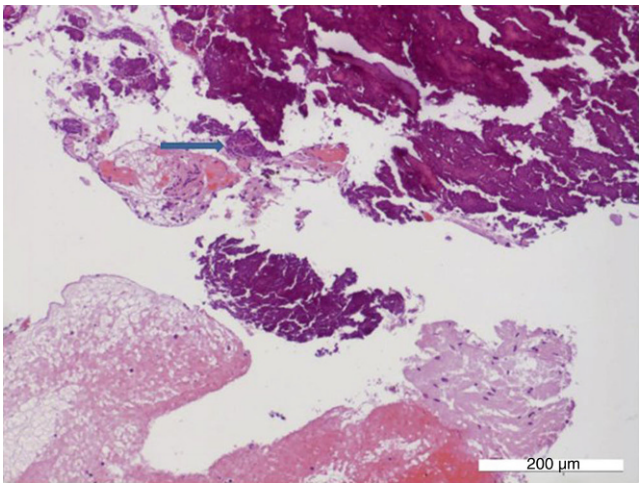

Fig. 6 Hematoxylin and eosin (H&E) staining shows calcified material, fresh coagulated blood, fibrin, gliotic and edematous CNS tissue, necrotic material and a small cell group consisting of mononuclear cells with a round nucleus (*arrow*), partly with artificial changes. Scale bar 200 µm

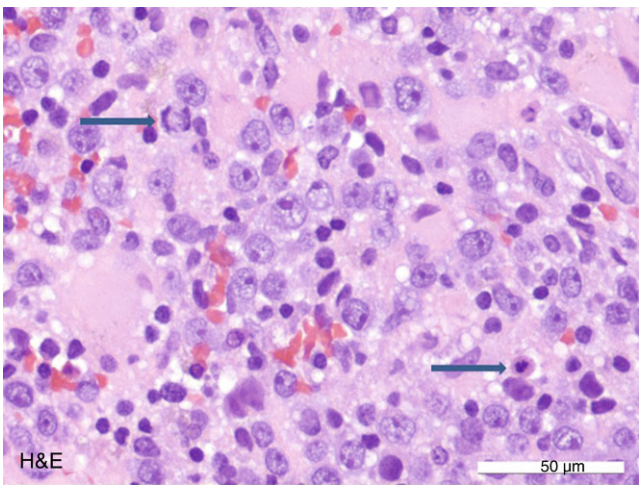

Fig. 7 Hematoxylin and eosin (H&E) staining displays cell-rich lymphoid tumor with dyshesive growth pattern, numerous large lymphoid cells with prominent nucleoli and isolated mitosis figures (*arrow*). Scale bars 50 µm

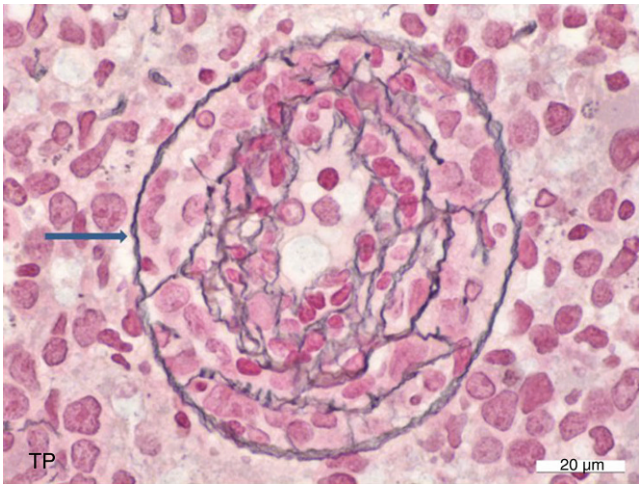

Fig. 8 Reticulin silver staining (Tibor Pap) displays an angiocentric growth pattern with concentric network and fragmentation of reticulin fibers (*arrow*) as well as perivascular accumulation of tumor cells. Scale bar 20 µm

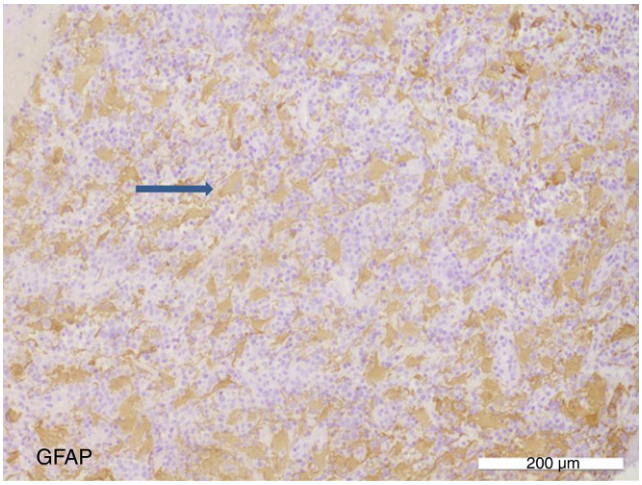

Fig. 9 On glial fibrillary acidic protein (GFAP) staining activated astrocytes are present in the local brain tissue (*arrow*). Scale bar 200 µm

lymphoid tumor with a dyshesive growth pattern. Numerous large lymphoid cells with prominent nucleoli could be detected in the tumor (Fig. 7). The cell nuclei were roundish-oval, partly hyperchromatic, and the cytoplasm appeared thin and eosinophilic. Regionally, an angiocentric growth pattern was also detectable (Fig. 8). Some mitotic and apoptotic figures could be seen in the tumor (Fig. 7). Many diffuse and partially vascularly associated small mature lymphocytes were found. The local gliotic brain tissue was partially diffuse and partially infiltrated by tumor cells along the blood vessels. Numerous activated astrocytes and microglial cells were detectable (Fig. 9). The tumor cells showed strong immunoreactivity for the pan B cell marker CD20 as well as for CD79a (Fig. 10a, b). Diffusely distributed and partly perivascularly emphasized, many small and mature reactive T cells were detected in the CD3 immunohistochemistry (Fig. 11). The CD68 labels several diffusely distributed macrophages. The proliferation rate in the MIB1 immunohistochemistry was very high (about 70%, Fig. 12). An Epstein-Barr virus (EBV) association could not be proven.

Figs. 7, 8, 9, 10, 11 and 12 relate to specimens from the second stereotactic biopsy.

Diagnosis

Malignant Diffuse Large B-Cell Lymphoma (DLBCL)

Primary CNS lymphomas (PCNSL) are highly proliferative B-cell neoplasms without a systemic manifestation. They are counted among the extranodal non-Hodgkin's

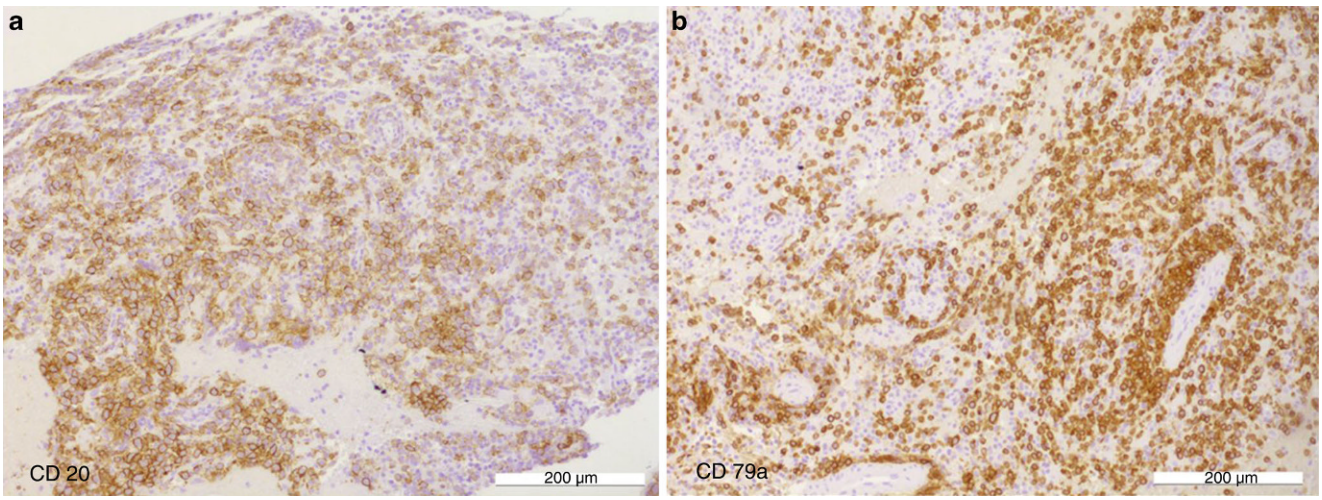

Fig. 10 CD 20 and CD 79a immunostaining shows tumor cell expression of the B-cell markers CD 20 (**a**) and CD 79a (**b**). Scale bars (**a, b**) 200 µm

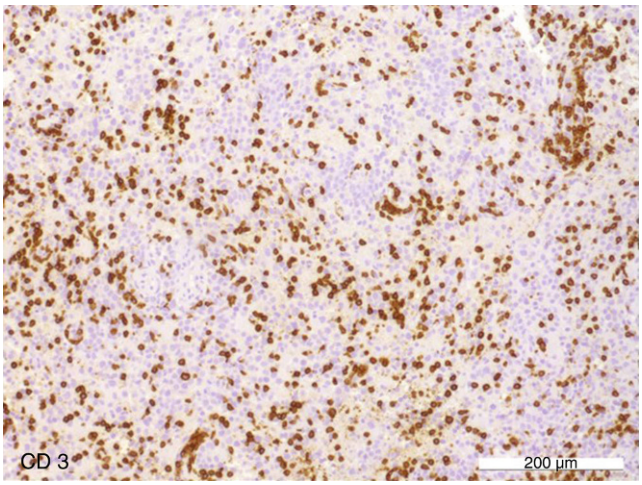

Fig. 11 CD 3 immunohistochemistry shows small and mature reactive T cells. Scale bar 200 µm

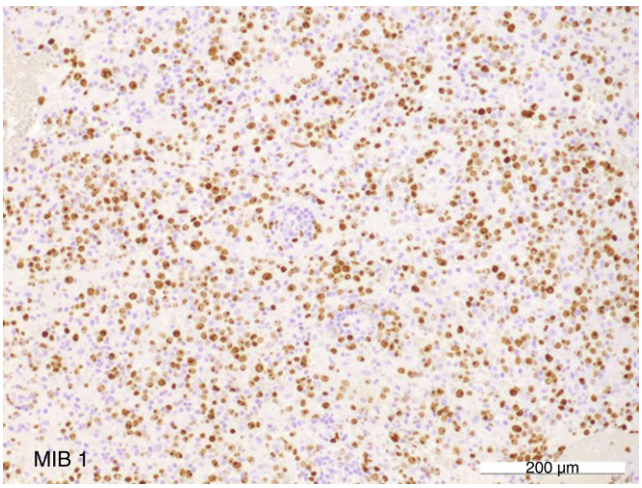

Fig. 12 In MIB1 immunohistochemistry a very high proliferation rate of the tumor can be seen. Scale bar 200 µm

lymphomas (NHL) and show an aggressive lawn-like infiltration of the brain parenchyma [10, 11]. With an incidence of 0.5:100,000, they represent 2.4–3% of all brain tumors and 4–6% of extranodal lymphomas [11, 12]. They can become manifested at any age. Patients in the 5th–7th decades are more frequently affected by an increasing incidence [11, 12]. Men are more affected than women (male-to-female ratio 3:2) [11, 18, 19]. In about 95% of all cases, PCNSL are classified as diffuse large B-cell type (DLBCL) and they are manifested largely in the supratentorial brain parenchyma. An infratentorial manifestation or a manifestation in the spinal cord is relatively rare. In about 10% of the cases the eyes are affected by retinal, uveal or vitreous infiltration (vitreoretinal lymphoma) [13–17]. In approximately 15% of the patients a leptomeningeal spread is described [12]. Immunosuppression is one of the risk factors for CNS lymphoma [12]. In general, such cases are EBV-associated [20]. Patient age (older than 65 years) and poor general condition are the major negative prognostic factors [11]. Higher levels of lactate dehydrogenase (LDH), increased cerebrospinal fluid (CSF) protein and deeper brain regions are also described as having a negative impact on prognosis [12].

The PCNSL are highly malignant neoplastic processes and have a considerably worse prognosis than systemic DLBCL [11]. In a purely symptomatic therapy, they have a median survival of weeks to a few months [12]. Under therapy, the 5-year survival rate is 31% [18]. The 2-year survival rate is 80% for low risk, 48% for medium risk and 15% for high risk patients [12, 22].

In clinical neuroradiologically suspected cases a minimally invasive stereotactic biopsy is indicated as the first choice for confirmation of the histological diagnosis. The role of neurosurgery is generally limited to sampling for definitive histological confirmation of the diagnosis. A surgical excision of the tumor alone is not considered to be sufficient treatment. It cannot be clearly stated whether a surgical tumor excision improves the prognosis. The PCNSL are radiation and chemotherapy sensitive tumors. The treatment of choice, however, is chemotherapy with blood-brain barrier adapted cytostatic agents. The PCNSL are very susceptible to steroid-induced apoptosis [11]. To ensure a reliable histological diagnosis, a steroid therapy before biopsy should be avoided as far as possible. Corticoid-mitigated lymphomas show microscopically only small numbers of neoplastic B-cells or no B-cells at all. They show non-specific inflammatory or reactive changes, often with necrosis and foamy macrophages [15, 21].

Compliance with ethical guidelines

Conflict of interest C.A. Taschner, S. Doostkam, P.C. Reinacher, H. Urbach, A. Rau and M. Prinz declare that they have no competing interests.

Ethical standards All investigations described in this manuscript were carried out with the approval of the responsible ethics committee and in accordance with national law and the Helsinki Declaration of 1975 (in its current revised form). Informed consent was obtained from the patient in this case if identifiable from images or other information within the manuscript.

References

1. Hebel R, Dubaniewicz-Wybieralska M, Dubaniewicz A. Overview of neurosarcoidosis: recent advances. J Neurol. 2015;262:258–67.
2. Ginat DT, Dhillon G, Almast J. Magnetic resonance imaging of neurosarcoidosis. J Clin Imaging Sci. 2011;1:15.
3. Black DF, Aksamit AJ, Morris JM. MR imaging of central nervous system Whipple disease: a 15-year review. AJNR Am J Neuroradiol. 2010;31:1493–7.
4. Kerbauy MN, Moraes FY, Lok BH, Ma J, Kerbauy LN, Spratt DE, et al. Challenges and opportunities in primary CNS lymphoma: a systematic review. Radiother Oncol. 2017;122:352–61.

5. Mansour A, Qandeel M, Abdel-Razeq H, Abu Ali HA. MR imaging features of intracranial primary CNS lymphoma in immune competent patients. Cancer Imaging. 2014;14:22.
6. Williams RL, Meltzer CC, Smirniotopoulos JG, Fukui MB, Inman M. Cerebral MR imaging in intravascular lymphomatosis. AJNR Am J Neuroradiol. 1998;19:427–31.
7. Martin-Duverneuil N, Mokhtari K, Behin A, Lafitte F, Hoang-Xuan K, Chiras J. Intravascular malignant lymphomatosis. Neuroradiology. 2002;44:749–54.
8. Taschner CA, Süß P, Sajonz B, Urbach H, Simon-Gabriel CP, Prinz M. Freiburg Neuropathology Case Conference : widespread white matter lesions in a patient with progressive paraparesis and cortical blindness. Clin Neuroradiol. 2017;27:245–50.
9. Taschner CA, Doostkam S, Shah JM, Urbach H, Jäger M, Prinz M. Freiburg Neuropathology Case Conference: cystic posterior fossa tumor. Clin Neuroradiol. 2017;27:393–8.
10. Schlegel U. Primary CNS lymphoma. Ther Adv Neurol Disord. 2009;2:93–104.
11. Louis DN, et al. WHO classification of tumours of the central nervous system. 4th ed. 2016.
12. Von Baumgarten L, Illerhaus G, Korfel A, Schlegel U, Deckert M, Dreyling M. The diagnosis and treatment of primary CNS lymphoma—an interdisciplinary challenge. Dtsch Ärztebl Int. 2018;115:419–26.
13. Korfel A, Schlegel U. Diagnosis and treatment of primary CNS lymphoma. Nat Rev Neurol. 2013;9:317–27.
14. Hoang-Xuan K, Bessell E, Bromberg J, Hottinger AF, Preusser M, Rudà R, et al. Diagnosis and treatment of primary CNS lymphoma in immunocompetent patients: guidelines from the European Association for Neuro-Oncology. Lancet Oncol. 2015;16:e322–32.
15. Deckert M, Brunn A, Montesinos-Rongen M, Terreni MR, Ponzoni M. Primary lymphoma of the central nervous system—a diagnostic challenge. Hematol Oncol. 2014;32:57–67.
16. Louis DN, Perry A, Reifenberger G, von Deimling A, Figarella-Branger D, Cavenee WK, et al. The 2016 world health organization classification of tumors of the central nervous system: a summary. Acta Neuropathol. 2016;131:803–20.
17. Hoffman S, Propp JM, McCarthy BJ. Temporal trends in incidence of primary brain tumors in the United States, 1985–1999. Neuro Oncol. 2006;8:27–37.
18. Shiels MS, Pfeiffer RM, Besson C, Clarke CA, Morton LM, Nogueira L, et al. Trends in primary central nervous system lymphoma incidence and survival in the U.S. Br J Haematol. 2016;174:417–24.
19. Mendez JS, Ostrom QT, Gittleman H, Kruchko C, DeAngelis LM, Barnholtz-Sloan JS, et al. The elderly left behind—changes in survival trends of primary central nervous system lymphoma over the past four decades. Neuro Oncol. 2018;20:687–94.
20. Deckert M, Engert A, Brück W, Ferreri AJ, Finke J, Illerhaus G, et al. Modern concepts in the biology, diagnosis, differential diagnosis and treatment of primary central nervous system lymphoma. Leukemia. 2011;25:1797–807.
21. Brück W Brunn A, Klapper W, Kuhlmann T, Metz I, Paulus W, et al. Differential diagnosis of lymphoid infiltrates in the central nervous system: experience of the network lymphomas and Lymphomatoid lesions in the nervous system. Pathologe. 2013;34:186–97.
22. Ferreri AJ, Blay JY, Reni M, Pasini F, Spina M, Ambrosetti A, et al. Prognostic scoring system for primary CNS lymphomas: the international extranodal lymphoma study group experience. J Clin Oncol. 2003;21:266–72.